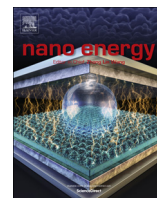




Contents lists available at ScienceDirect

Nano Energy

journal homepage: www.elsevier.com/locate/nanoen

Dimethyl ether electro-oxidation on platinum surfaces

Luke T. Roling, Jeffrey A. Herron, Winny Budiman, Peter Ferrin, Manos Mavrikakis*

Department of Chemical and Biological Engineering, University of Wisconsin – Madison, 1415 Engineering Drive, Madison, WI 53706, United States

ARTICLE INFO

Article history:

Received 22 December 2015

Received in revised form

5 February 2016

Accepted 20 February 2016

Keywords:

Dimethyl ether

Transition metals

Fuel cell

Structure sensitivity

Density functional theory

ABSTRACT

A first-principles density functional theory study was performed to elucidate the mechanism of dimethyl ether electro-oxidation on three low-index platinum surfaces (Pt(111), Pt(100), and Pt(211)). The goal of this study is to provide a fundamental explanation for the high activity observed experimentally on Pt(100) compared to Pt(111) and stepped surfaces. We determine that the enhanced activity of Pt(100) stems from more facile C–O bond breaking kinetics, as well as from easier removal of CO as a surface poison through activation of water. In general, the C–O bond (in CH_xOCH_y) becomes easier to break as dimethyl ether is dehydrogenated to a greater extent. In contrast, dehydrogenation becomes more difficult as more hydrogen atoms are removed. We perform two analyses of probable reaction pathways, which both identify CHOC and CO as the key reaction intermediates on these Pt surfaces. We show that the reaction mechanism on each surface is dependent on the cell operating potential, as increasing the potential facilitates C–H bond scission, in turn promoting the formation of intermediates for which C–O scission is more facile. We additionally demonstrate that CO oxidation determines the high overpotential required for electro-oxidation on Pt surfaces. At practical operating potentials ($\sim 0.60 V_{\text{RHE}}$), we determine that C–O bond breaking is most likely the most difficult step on all three Pt surfaces studied.

© 2016 Elsevier Ltd. All rights reserved.

1. Introduction

Dimethyl ether (DME) has attracted substantial interest as an alternative fuel, primarily as an additive in gasoline or diesel fuels. However, DME has also demonstrated potential as a feed for low temperature proton exchange membrane (PEM) fuel cells. DME is readily produced from the dehydration of methanol [1]. Its physical properties are similar to those of liquefied petroleum gas, and it therefore can be stored and transported utilizing existing infrastructures [2], making it an attractive alternative fuel for rapid integration into portable fuel markets. DME has other key advantages over other fuel cell feeds. DME is stored and transported as a liquid, a clear benefit over hydrogen gas. No C–C bond cleavage is required, as in ethanol oxidation, which makes complete oxidation of DME to CO_2 more facile [3]. Further, DME is nontoxic and exhibits a significantly reduced crossover effect to the cathode [4], both key advantages over methanol, another promising low-temperature fuel cell feed. DME electro-oxidation has an equilibrium voltage of 1.20 V, which compares favorably with those of methanol (1.21 V), ethanol (1.15 V), and hydrogen (1.23 V) [5].

Despite the aforementioned advantages of DME, its electro-oxidation reaction has not been well characterized, and relatively few attempts have been made to optimize the catalyst for this

reaction. These studies have focused primarily on Pt-based alloys, such as PtRu and PtSn [3,6], that demonstrate promise for methanol electro-oxidation, which shares common mechanistic steps with the DME electro-oxidation network. Li and coworkers recently presented a ternary Pt–Pd–Ru catalyst with improved DME electro-oxidation activity, which was rationalized by reduced calculated activation energy barriers to C–O and C–H bond breaking in DME relative to PtRu(111) and Pt(111) [7]. CO poisoning is a well-known problem on Pt electrodes during DME electro-oxidation [8], but the mechanisms by which CO forms and is removed have not been fully elucidated.

DME electro-oxidation has been shown to have significant structure sensitivity on Pt catalysts, and CO has been hypothesized as a possible cause of the observed sensitivity. Osawa, Ye, and coworkers have suggested that Pt(100) produces CO_2 through a direct mechanism (no partial oxidation products), while the Pt(111) facet is only active via an indirect mechanism through forming surface CO [9–11]. They found that the primary DME electro-oxidation peak occurs at roughly $0.8 V_{\text{RHE}}$ on Pt(111), while a more active peak is found at slightly less than $0.7 V_{\text{RHE}}$ on Pt(100), demonstrating the improved performance of Pt(100). Koper and colleagues have conducted experiments and performed DFT calculations on Pt(100), Pt(510), and Pt(10 1 0), which are stepped surfaces with large (100) terraces [12]. Their results show that the stepped surfaces are less active than pure Pt(100) electrodes, in part because they restrict the ability to form adsorbed CO from adsorbed CH_x species. They also conclude that C–O bond cleavage

* Corresponding author.

E-mail address: manos@engr.wisc.edu (M. Mavrikakis).

to CH and CO occurs through the CHOC intermediate, which is stabilized by symmetry on (100) terraces but not on the step edges. Therefore, they predict that the coverage of CHOC on step edges would be too low for steps to contribute significantly to the C–O bond breaking events.

In previous work, we studied the structure sensitivity of DME electro-oxidation thermochemistry on the (111) and (100) facets of eight transition metal surfaces [13,14]. In general, we found that the thermochemistry of C–O bond scission was more favorable on the (100) facets, which was facilitated by the relative ease of dehydrogenation on these surfaces. In particular, we found that Pt(100) has lower thermochemical barriers to full oxidation to CO₂ than does Pt(111), in agreement with the observations of Osawa and Ye [9–11]. However, those studies did not consider the activation energy barrier, i.e., kinetics, of C–O bond scission, relying only on thermodynamic arguments.

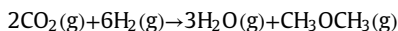
In the present study, we extend our understanding of the structure sensitivity of the DME electro-oxidation reaction on Pt surfaces by reporting the kinetic barriers for C–O bond scission on Pt(111), Pt(100), and Pt(211). We postulate likely reaction mechanisms on each surface, and identify fundamental reasons for the observed high activity of Pt(100) compared to Pt(111) and Pt(211). Our detailed reaction mechanisms provide an atomic-scale explanation for the observed structure sensitivity of DME electro-oxidation on Pt single crystal surfaces, simultaneously demonstrating that the reaction mechanisms depend on the cell operating potential.

2. Methods

The free energies of all reaction species are calculated using density functional theory (DFT) as implemented in DACAPO [15,16], a total energy code. Calculations are performed on the Pt(111), Pt(100), and Pt(211) facets. The Pt(111) surface is represented by a periodic 3 × 3 unit cell with three layers of metal atoms fixed at their bulk positions, in accordance with previous calculations showing that relaxation effects on Pt(111) are minimal [17,18]. The Pt(100) surface is modeled using a periodic 3 × 3 unit cell with four layers of metal atoms; the atoms in the top two layers are fully relaxed, while the bottom two layers are fixed at their bulk positions. The Pt(211) surface is modeled with a periodic 1 × 3 unit cell with nine layers of metal atoms; the bottom five layers are fixed at their bulk positions, while the top four layers are allowed to relax. At least 10 Å of vacuum separate successive slabs of each facet. The optimized Pt lattice constant was calculated to be 4.00 Å, in good agreement with the experimental value of 3.92 Å [19]. Adsorption is permitted on only one exposed surface, with the dipole moment corrected accordingly [20,21]. The Kohn–Sham one-electron states are expanded in a basis of plane waves with an energy cutoff of 25 Rydberg, and the ionic cores are described using ultrasoft Vanderbilt pseudopotentials [22]. The surface Brillouin zone of the Pt(111) facet is sampled with 18 special Chadi–Cohen *k*-points [23], and the Pt(100) and Pt(211) facets are sampled with a 4 × 4 × 1 Monkhorst–Pack *k*-point mesh [24]. The exchange–correlation energy and potential are described self-consistently using the GGA-PW91 functional [25]. The electron density is determined by iterative diagonalization of the Kohn–Sham Hamiltonian, Fermi population of the Kohn–Sham states (*k_BT* = 0.1 eV), and the Pulay mixing of the resulting electronic density. All total energies are extrapolated to *k_BT* = 0 eV. The convergence of binding energies with respect to the various calculation parameters was verified. Activation energy barriers are calculated using the climbing image nudged elastic band (CI-NEB) method [26]. The calculated transition states were verified by vibrational frequency analysis to confirm the existence of one imaginary vibrational mode.

The zero-point energy (ZPE) correction is included in the free energy of all adsorbates, calculated by assuming a quantum harmonic oscillator with calculated vibrational frequencies, which are calculated by numerical differentiation of forces using a second-order finite difference approach with a step size of 0.015 Å [27]. Vibrational frequencies and modes were calculated by mass-weighting and diagonalization of the Hessian matrix. The calculated entropy of all surface species includes translational, vibrational, and rotational modes.

All gas-phase free energies are calculated relative to the DFT-derived energies of H₂O(g), CO₂(g), and H₂(g). For example, the energy of gas-phase DME is determined from the following reaction:



from which the free energy of DME can be calculated as:

$$G_{\text{CH}_3\text{OCH}_3} = (E_{\text{CH}_3\text{OCH}_3} - TS_{\text{CH}_3\text{OCH}_3} + ZPE_{\text{CH}_3\text{OCH}_3}) + 3(E_{\text{H}_2\text{O}} - TS_{\text{H}_2\text{O}} + ZPE_{\text{H}_2\text{O}}) - 6(E_{\text{H}_2} - TS_{\text{H}_2} + ZPE_{\text{H}_2}) - 2(E_{\text{CO}_2} - TS_{\text{CO}_2} + ZPE_{\text{CO}_2})$$

where *E* is the total energy of a species calculated from DFT, *T* is the standard temperature (298 K), *S* is the calculated entropy and *ZPE* is the calculated zero-point energy for the species. The total energy of adsorbed species is taken relative to the gas-phase species and clean surface, while *S* and *ZPE* are calculated for the adsorbed state. The free energies of all C–O bond scission steps are calculated with the products at infinite separation.

To account for the effect of the electrochemical potential on the free energies of adsorbed species, we employ the computational hydrogen electrode developed by Nørskov and coworkers [28]. We first take the electrochemical reference to be the reversible hydrogen electrode (RHE), in which H₂ gas is in equilibrium with protons and electrons according to the reaction H₂ ↔ 2(H⁺ + e[−]) at all pH, 298 K, and 1 atm pressure of H₂ at a defined potential of 0.00 V_{RHE}. The change in free energy of proton–electron transfer steps was therefore calculated as Δ*G* = Δ*E* + Δ*ZPE* − *T*Δ*S* − |*e*|*U*, where |*e*| is the absolute charge of an electron and *U* is the electrochemical operating potential versus the RHE. An increase in the electrode potential by *U* will therefore make the proton–electron transfer more favorable by −|*e*|*U*. This potential correction term only affects the free energy of electrochemical reaction steps; the free energies of C–O bond breaking events are therefore left unchanged. All values of cell potential reported in this work are given in reference to the RHE; we omit this distinction hereafter for brevity.

We recognize some limitations of our model, particularly regarding conditions of this study that may vary from those present in the experimental reaction environment. All thermochemistry is calculated at 1/9 ML surface coverage, which may differ from the true surface environment under different electrochemical conditions and could significantly impact the agreement between theory and experiment. We also neglect any contributions to the free energies of adsorbed species from water molecules of the electrolyte, which have been shown to stabilize adsorbed OH on the surface [29–32]. We anticipate that solvation could stabilize other intermediates with similar chemical functionalities, and thus omit all solvation effects in the absence of a systematic study of such effects in this study (or in the literature) to avoid biasing the results based on stabilizing only OH. Nevertheless, we believe that our model provides a reasonable explanation of the experimental observations, whereas the fundamental insights gained into the reaction mechanism can inform future catalyst design for this reaction.

Download English Version:

<https://daneshyari.com/en/article/5452577>

Download Persian Version:

<https://daneshyari.com/article/5452577>

[Daneshyari.com](https://daneshyari.com)